JOURNAL OF AIRCRAFT
Vol. 37, No. 5, September–October 2000

Use of Strip Yield Approach for Multiple-Site Damage Failure Scenarios

J. H. Kuang*
National Sun Yat-Sen University, Kaohsiung 80424, Taiwan, Republic of China
and
C. K. Chen†
Metal Industries Research and Developments Center, Kaohsiung 80424, Taiwan, Republic of China

With the embodiment of Dugdale's plastic zone model (Dugdale, D. S., "Yielding of Steel Sheets Containing Slits," *Journal of Mechanics and Physics of Solids*, Vol. 8, No. 2, 1960, pp. 100–104) and Swift's link-up criterion (Swift, T., "Damage Tolerance Capability," *Fatigue of Aircraft Materials*, Delft Univ. Press, Delft, The Netherlands, 1992, pp. 351–387), an alternating iteration method is used for solving multiple-site damage (MSD) cracking problems. The crack tip opening displacement at the main crack tip is also suggested to assess ligament failure scenarios for different MSD panels under their corresponding link-up stresses. Predictions of multiple-crack link-up can be obtained to give reasonable agreement with published experimental data.

Introduction

AFTER the Aloha Airlines accident[1] in April 1988, the significant impact of multiple-site damage (MSD) became a great concern. A uniform stress field prevails in the fuselage structure and the MSD cracks generally emanate from several adjacent and collinear rivet holes in the longitudinal fuselage skin splice. The fracture characteristics of MSD are significantly different from the characteristics of a single-site crack. The different failure scenarios for a lead crack and neighboring smaller MSD cracks, as discussed by Schijve,[2] show that small MSD cracks can significantly reduce the failure load for unstable crack extension. The sudden coalescence of MSD may lead to a single critical crack that can cause catastrophic failure of a fuselage structure. Therefore, the understanding of complex MSD failure scenarios are crucial for fail-safe structural design. In addition, this can also provide for the prevention of catastrophic consequences resulting from inadequate MSD crack arresting methods.

The fuselages of many airplanes are constructed of thin 2024-T3 Alclad sheets with thickness ranging from 0.8 to 2 mm. The ductility of the 2024-T3 material will result in large-scale plastic deformation at the crack tips. Unless depiction of the interaction between the plastic zones of adjacent cracks can be drawn, recognition of MSD fractures and failure scenarios can not be fully clear. The conventional stress intensity factor, which results from the small scale yielding assumption, is restricted in the application of fracture of ductile materials. Therefore, failure criteria based on local crack tip deformation characteristics (i.e., crack tip opening angle[3] (CTOA) and T^* integrals[4]) were employed to predict the MSD failure scenario of thin sheet structure. The predictions are promising, but extensive and tedious calculations must be utilized. Thus, an engineering approach using the failure criterion of crack tip opening displacement (CTOD) and plastic zone coalescence is proposed to determine the failure scenario for a multiple-cracked sheet structure. Dugdale's plastic zone correction[5] is employed in the calculation of multiple crack interaction.

In this paper, symmetric MSD with a leading crack is evaluated by an alternating technique. Multiple cracks' stress reflections are also included in the examination. The alternating iteration process can reach accurate stress patterns around multiple-crack tips. Moreover, the yield strip sizes forward of crack tips are concurrently calculated in the iterative process by their approaching the condition of vanishing stress intensity factors at Dugdale crack tips. Swift's intuitive model[6] proposes that two cracks are linked up as the adjacent plastic zones coalesce. The rupture of MSD cracks may initiate in two possible ways: rupture from the leading crack tip directly, or link-up between the lead crack and neighboring small MSD crack first and then a rupture emanating from the absorbed crack tip. The crack absorption, however, may be in a stable or unstable process. The critical value of CTOD at the physical crack tip under the link-up load is employed herein to assess the stability process for MSD cracking. The availability of using CTOD to predict the type of failure is examined with published experimental data.[7] Accordingly, the failure scenario for MSD thin sheet structures can be predicted.

Received 24 May 1999; revision received 9 March 2000; accepted for publication 11 March 2000.

*Professor, Department of Mechanical Engineering.
†Research Engineer, Metal Forming Technology Section.

Results of the Flat Panels

The residual strengths of flat MSD panels were analyzed by Broek et al.[7] The 2024-T3 thin flat panels were monotonically loaded in the uniaxial direction, where the panel width is 508 mm, length is 1016 mm, and thickness is 1 mm. Three panels (P1, P2, and P3) have a single crack, and nine panels possess a central leading crack accompanied by neighboring small MSD cracks. The MSD cracks are collinearly aligned with the leading crack. The cracking patterns for these twelve flat panels are presented in Fig. 1, because all the small MSD are symmetric with the central leading crack, such that only half of the cracked configurations are shown. Figure 1 also lists the stresses at link up and at rupture. Results indicate that some panel failures and link up may occur simultaneously. *F* denotes this MSD failure in Fig. 1. However, in some cases, no crack rupture was observed under the link-up load. A so-called crack absorption (*A* in Fig. 1) was used herein to specify such MSD status. Cracks are temporarily arrested during crack absorption, and an additional increase of the load is necessary to induce panel failure. Results indicate that a significant strength loss may occur for different MSD configurations. Note how profusely the MSD cracks can affect the leading crack. Failure scenarios are subjected to be alternated, that is, direct MSD panel rupture or MSD crack absorption, depending on different MSD configurations. The behavior of the leading crack with MSD must be clarified because this type of damage is widely experienced in the aircraft industry. In addition, clarification of MSD failure modes will enhance worldwide aircraft inspection programs.

Computation for MSD Cracks

Strip Yield Model

A strip yield model accounting for the spreading of plasticity ahead of the crack tip, in plane stress condition of a thin sheet,

had been introduced by Dugdale.[5] This model assumes the material follows elastic, perfectly plastic behavior that obeys Tresca yield criterion. The plastic zones of Dugdale cracks are assumed to be a type of cross-slip mode on planes that subtend 45 deg to the plane of the sheet. The plastic zone size of a typical Dugdale crack is calculated by treating the real crack length along with an unknown adjacent plastic zone as an elastic crack. In the examination of crack interaction, the Dugdale strip yield model is employed in numerical calculations. Figure 2 shows the Dugdale yield model for three symmetric collinear cracks under a uniform remote stress σ^{∞}. Three symmetric collinear aligned cracks have leading crack lengths of $2a_M$ and two neighboring MSD of $2a_S$, respectively. The original multiple crack problem is decomposed into two subproblems by extending Dugdale's strip yield model. σ_{ys} denotes the yield strength of the material. ρ_M, ρ_{S1}, and ρ_{S2} are undetermined plastic zones ahead of real cracks. The artificial elastic crack is loaded remotely by a uniform stress and a set of yielding strengths acting uniformly along the plastic zones. The half-lengths of cracks are

$$c_M = a_M + \rho_M \tag{1}$$

$$c_S = (2a_S + \rho_{S1} + \rho_{S2})/2 \tag{2}$$

In the iterative calculation mentioned hereafter, the undetermined plastic damage zones (ρ_M, ρ_{S1}, and ρ_{S2}) are preassumed in a trial-and-error sense. The problem is then solved with the Dugdale approach. The stress intensity factors at artificial crack tips in Figs. 2b and 2c must be equal in magnitude for the corresponding crack tips. For the symmetric condition displayed in Fig. 3, only the stress intensity factors at the artificial crack tips 1, 2, and 3 need to be evaluated. In Fig. 2b, the stress intensity factors at the leading crack and neighboring small cracks are, for crack tip 1

$$K_{I\sigma^{\infty}}^{(1)} = \sigma^{\infty}\sqrt{\pi c_M} f_1(c_M, c_S, d) \tag{3}$$

for crack tip 2

$$K_{I\sigma^{\infty}}^{(2)} = \sigma^{\infty}\sqrt{\pi c_S} f_2(c_M, c_S, d) \tag{4}$$

and for crack tip 3

$$K_{I\sigma^{\infty}}^{(3)} = \sigma^{\infty}\sqrt{\pi c_S} f_3(c_M, c_S, d) \tag{5}$$

Those for Fig. 2c are, for crack tip 1

$$K_{I\sigma_{ys}}^{(1)} = \sigma_{ys}\sqrt{\pi c_M} g_1(a_M, a_S, \rho_M, \rho_{S1}, \rho_{S2}, d) \tag{6}$$

for crack tip 2

$$K_{I\sigma_{ys}}^{(2)} = \sigma_{ys}\sqrt{\pi c_S} g_2(a_M, a_S, \rho_M, \rho_{S1}, \rho_{S2}, d) \tag{7}$$

for crack tip 3

$$K_{I\sigma_{ys}}^{(3)} = \sigma_{ys}\sqrt{\pi c_S} g_3(a_M, a_S, \rho_M, \rho_{S1}, \rho_{S2}, d) \tag{8}$$

where f_i and g_i are numerically defined functions. In Dugdale's approach,[5] the stress intensity factors at crack tips 1, 2, and 3 in Figs. 2b and 2c must be equal in magnitude, that is, $K_{I\sigma^{\infty}}^{(1)} = K_{I\sigma_{ys}}^{(1)}$, $K_{I\sigma^{\infty}}^{(2)} = K_{I\sigma_{ys}}^{(2)}$, and $K_{I\sigma^{\infty}}^{(3)} = K_{I\sigma_{ys}}^{(3)}$. This leads to

$$g_1/f_1 = g_2/f_2 = g_3/f_3 = \sigma^{\infty}/\sigma_{ys} \tag{9}$$

Eq. (9) serves as checking criteria for the preassumed values of the Dugdale plastic damage zones ρ_M, ρ_{S1}, and ρ_{S2} in the alternating iteration process discussed hereafter.

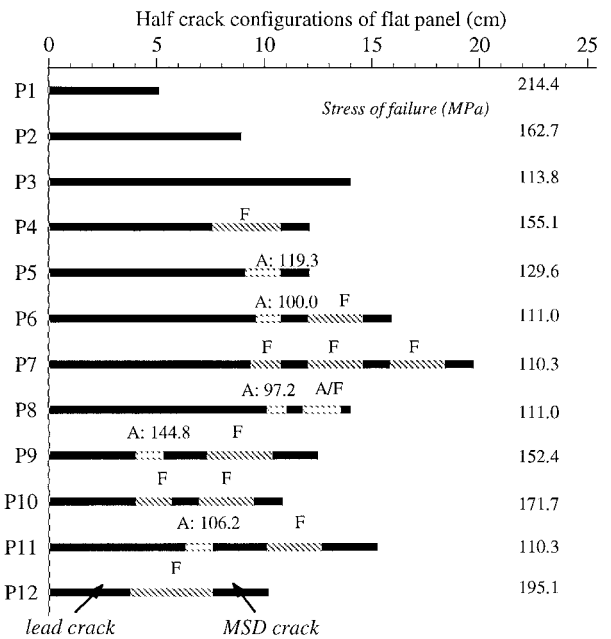

Fig. 1 Configurations of test panels in Ref. 7.

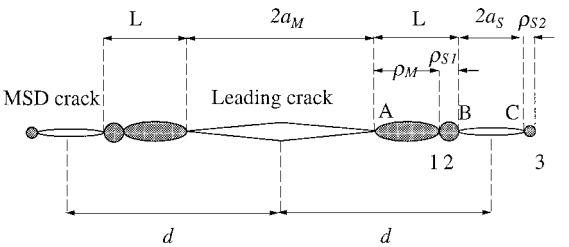

Fig. 3 Schematic representation of Swift's[6] intuitive model.

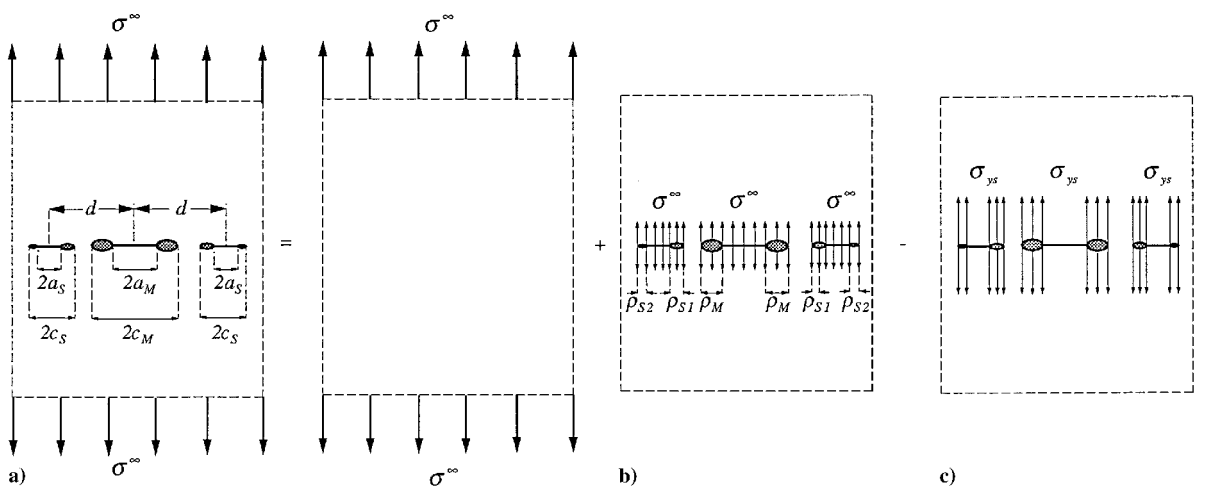

Fig. 2 Dugdale's[5] strip yielding model for three symmetric collinear cracks.

Alternating Iteration Method

Two subproblems of Figs. 2b and 2c are solved individually using the method of alternating iteration[8,9] to free their own crack surface traction. In each loading system, stress distributions on the imaginary position of cracks are calculated by using respective Westergaard stress functions (see Ref. 10). Whereas only one crack exists in the calculation, the remaining cracks are considered imaginary cracks. For numerical convenience, constant tractions on imaginary positions are averaged along each crack length. Distributed stresses shed on the domain are, thus, derived approximately from these constant tractions. The stress field with negative traction on each imaginary crack is then imposed onto the existing stress field to free crack surface traction. In doing so, new image traction may be introduced to the once image-traction-free crack. These residual image tractions are successively reduced by the repeated alternating iteration. A similar process is repeated until the residual image traction on all three cracks approach zero simultaneously. There is an obvious advantage to this iteration method, in which the interaction effect between cracks has been particularly considered. The imaginary traction on the free surfaces of a prospective crack could then be imposed in every iteration cycle. Therefore, the kth increment of stress intensity factors at an artificial crack tip $[\Delta K_I^k(\pm c_j)]$ owing to mutual crack interaction can be integrated from the concentrated force results provided in Ref. 10 and displayed in Eq. (10):

$$\Delta K_I^k(\pm c_j) = \frac{1}{\sqrt{\pi c_j}} \int_{-c_j}^{c_j} p_j^k(\xi_j) \sqrt{\frac{c_j \pm \xi_j}{c_j \mp \xi_j}}\, \mathrm{d}\xi_j \qquad j = M, S \tag{10}$$

where $p_j^k(\xi_j)$ is the image stress function distributed along the c_j crack in the kth iteration. Stress intensity factor solutions are employed in the plastic zone verifying procedure as mentioned in Eq. (9). Hence, assumed plastic zones ahead of each crack tip can be assured. In addition, the increment for crack tip opening displacement at the physical crack tip $[\Delta \delta_t^k(\pm a_j)]$ for each iteration can also be calculated in Eq. (11). The equation is integrated from the CTOD result for a pair of normal concentrated forces acting on the crack surface as described in Ref. 10:

$$\Delta \delta_t^k(\pm a_j) = \frac{4}{E\pi} \int_{-c_j}^{c_j} p_j^k(\xi_j) \cosh^{-1}\left(\frac{c_j^2 - a_j' \xi_j}{c_j |\xi_j - a_j'|} \right) \mathrm{d}\xi_j \qquad j = M, S \tag{11}$$

In which E denotes Young's modulus. Furthermore, a_j' is shown in Eqs. (12) and (13):

$$a_M' = \pm a_M \tag{12}$$

$$a_S' = \pm a_S - (\rho_{S1} - \rho_{S2})/2 \tag{13}$$

The solutions of Figs. 2b and 2c are reached by superposing their own initial solution and successive solutions in every iteration. To avoid the link-up singularity difficulty in the proposed iterative calculation, cracks are considered linked as inner plastic zones separated by minute distances ($\varepsilon = L/100$)

Ligament Failure Scenario for MSD Thin Panels

The failure scenarios of MSD panels are simulated by the plastic zones contact for adjacent cracks. Experimental observations[7] indicate that the rupture of MSD panels may prevail either at the leading crack tip or at the absorbed crack tip. The CTOD at the main crack tip is employed in this paper to distinguish the direct ligament rupture from the absorption failure in MSD cracking problems. It is proposed that, in the instance of neighboring plastic zones link up, the ligament failure will initiate from the leading crack tip if the CTOD δ_t of the main crack tip exceeds the corresponding critical CTOD value δ_t^c of this panel. It is proposed that the direct MSD rupture prevails only as the CTOD δ_t at leading crack is over δ_t^c. On the contrary, if the CTOD δ_t under the link-up stress is less than δ_t^c, a crack absorption of adjacent cracks may occur. The linked cracks are considered to function as a single crack. It is then assumed that the stability of this crack absorption is determined on the δ_t^* at the absorbed crack tip. The crack absorption is unstable as the δ_t^* at the absorbed crack tip is over δ_t^c. The flow chart shown in Fig. 4 illustrates the proposed scheme for MSD rupture and/or absorption identification. To show the availability of this identification scheme, the ligament failure scenarios of the MSD tests[7] are evaluated.

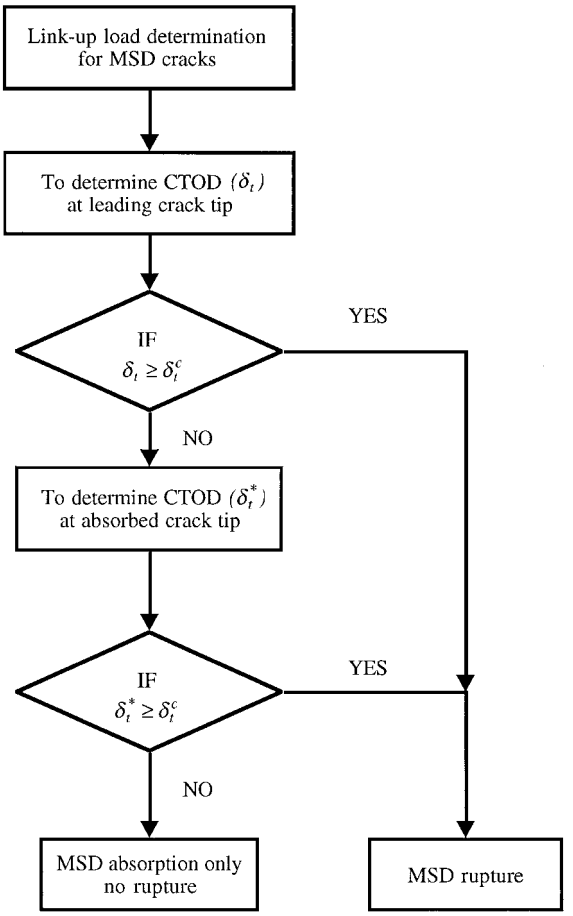

Fig. 4 Flow chart of the determination of MSD absorption/rupture.

Critical CTOD Values for 2024-T3 MSD Panels

The test results of P1, P2, and P3 shown in Fig. 1 are considered central cracked panels. In the case of a specimen with limited sheet thickness, one can express the apparent fracture toughness K_c of this specimen in terms of geometric parameters and loading stress in the form

$$K_c = \beta_w \sigma_c \sqrt{\pi a} \tag{14}$$

Here, β_w is the geometric coefficient[10] for a center crack of length $2a$, in a plate width of W, which is depicted in Eq. (15) wherein σ_c denotes critical remote applied stress:

$$\beta_w = \sqrt{\sec(\pi a / W)} \tag{15}$$

K_c for these 2024-T3 MSD panels is calculated to be 90 MPa $\sqrt{m}$, which is averaged from results in the P1–P3 cases. On the other hand, Hoysan and Sinclare[11] take the apparent fracture toughness of this material to be 110 MPa $\sqrt{m}$. In this paper, nevertheless, K_c is assigned to be 100 MPa $\sqrt{m}$, which is consistent with the same material with identical thickness provided in Ref. 4. The other mechanical properties of the 2024-T3 Alclad sheet[12] are Young's modulus $E = 71{,}400$ MPa, yield strength $\sigma_{ys} = 344$ MPa, and tensile strength

Table 1 Failure scenarios of different MSD panels under their first link-up loads

Specimen	Crack dimensions, mm			Plastic zone sizes, mm			CTOD, $(\delta_t)_A$, mm	σ^*_∞, MPa	Experimental result
	a_M	L	a_S	ρ_M	ρ_{S1}	ρ_{S2}			
P4	76.2	31.8	6.3	25.3	6.5	4.6	0.407	170.9	F
P5	91.4	16.6	6.3	12.7	3.9	2.5	0.284	119.3	A
P6	96.5	11.4	6.3	8.5	2.9	1.8	0.246	90.3	A
P7	94.0	14.0	6.3	10.0	4.0	2.2	0.465	103.0	F
P8	101.6	8.9	3.8	6.9	2.0	1.2	0.215	81.4	A
P9	40.6	12.7	10.2	8.8	3.9	2.6	0.165	124.8	A
P10	40.6	16.5	6.4	12.2	4.3	3.0	0.239	156.1	F
P11	63.5	12.7	12.7	8.8	3.9	2.5	0.329	101.7	A
P12	38.1	38.1	12.7	26.5	11.6	9.0	0.386	211.0	F

Table 2 Failure scenarios of specimens P6, P8, P9, and P11 under their second link-up loads

Specimen	Crack dimensions, mm			Plastic zone sizes, mm			CTOD, $(\delta_t)_A$, mm	σ^*_∞, MPa	Experimental result
	a_M	L	a_S	ρ_M	ρ_{S1}	ρ_{S2}			
P6	120.7	25.4	6.3	20.0	5.4	3.6	0.478	128.7	F
P8	118.1	17.8	3.8	14.5	3.3	2.2	0.351	112.8	A/F
P9	73.7	30.5	10.2	22.7	7.8	5.6	0.421	161.7	F
P11	101.6	25.4	12.7	18.6	6.8	4.6	1.115	126.7	F

$\sigma_{ult} = 462$ MPa. The associated critical CTOD $\delta_t^c = 0.35$ mm is evaluated from Eq. (16):

$$\delta_t^c = K_c^2 \Big/ E\sigma_{flow} \tag{16}$$

where flow strength of 2024 Alclad is defined in the following equation and is 403 MPa:

$$\sigma_{flow} = (\sigma_{ys} + \sigma_{ult})/2 \tag{17}$$

Correlation of Test Results with Analysis

The MSD tests P4–P12 in Ref. 7 are analyzed with the strip model and alternative iteration mentioned earlier. Swift's[6] link-up criterion, as shown in Fig. 3, is employed to predict link-up loads for multiple-cracked 2024-T3 aluminum thin panels. Thus, solutions for the applied coalescence stress and the unknown Dugdale[5] plastic zones ahead of crack tips can be evaluated. Results are given in Table 1 for the first link up of MSD. In the instance of the adjacent plastic zone coalescence, the CTOD $(\delta_t)_A$ at the physical main crack tip A shown in Fig. 3 may exceed the critical CTOD δ_t^c (0.35 mm), that is, as presented in cases of P4, P7, and P12. In these cases, a direct MSD rupture is initiated from the tip of the leading crack as the load increases up to the link-up stress σ^*_∞. F is used in Fig. 1 and Table 1 to denote this type MSD failure in experiments. In these tests, case P10 shows $(\delta_t)_A < \delta_t^c$ at the leading crack tip but $\delta_t^* > \delta_t^c$ at the absorbed crack tip under the link-up load. As mentioned, an unstable crack absorption can take place in such a case and a final MSD rupture may occur following the crack absorption. A stable crack absorption at the link-up load prevails for cases of P5, P6 , P8, P9, and P11. Values of $(\delta_t)_A$ and δ_t^* are both less than the critical δ_t^c in these cases. A further load must be applied to introduce the second link up or rupture.

Failure scenarios for the second link up are listed in Table 2, whereas the empirical failure scenario corresponds to the predicted results. In the second link up, an ambiguous stability is observed for case of P8, which can be expected from the calculated data. Numerical results in the second plastic zones link up reveal that the CTOD $(\delta_t)_A$ is very close to the critical δ_t^c. Thus, observation difficulty may prevail in such a testing configuration. Link-up stresses σ^*_∞ for different MSD configurations have been computed in the corresponding numerical iterations and are listed in Tables 1 and 2. In the evaluation of the link-up stress, the material flow strength is assumed to account for the strain hardening effect in experiments.

Figure 5 shows the comparison of estimated link-up stresses and the measured results. The percentage difference between predictions and measured link-up stresses is between −16.3 and 15.9%. The absolute average percentage error for all the estimated link-up stresses is about 9%, which is within an acceptable experimental deviation. The correlation between the measured and the calculated MSD failure scenarios reveals that the proposed method can be employed to analyze the MSD problems with good accuracy. It is believed that the consideration of crack interaction with strip yield model is the key reason for obtaining such good results. Results also indicate that the CTOD at the leading crack tip or the absorbed crack tip can be used to predict the possible MSD failure scenario successfully.

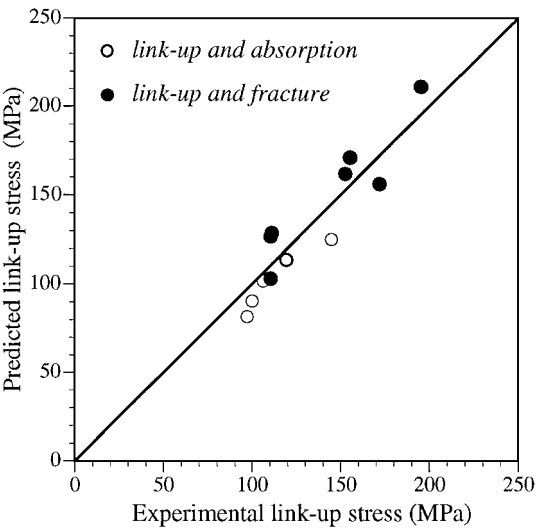

Fig. 5 Comparison of predicted and measured link-up stresses.

Conclusions

1) With Dugdale's[5] strip yield model and Swift's[6] link up criterion, an alternating iteration method can be utilized to predict the link-up phenomenon in MSD failure. The absolute averaged percentage difference between predictions and measured link-up stress is about 9%.

2) The value of CTOD at the link-up load can be used to examine whether a stable crack absorption or a direct rupture may occur in MSD cracking problems. Results from multiple cracked 2024-T3 thin panels indicate that a good correlation is reached between the measured and the predicted MSD failure scenarios.

3) Consideration of the interaction between cracks appears to affect the accuracy of predictions for MSD link up.

Acknowledgments

The authors would like to thank the National Science Council, Taiwan, Republic of China, for financially supporting this research through Grant NSC82-0401-E-110-032.

References

[1]Hendricks, W. R., "The Aloha Airlines Accident—A New Era for Aging Aircraft," *Structural Integrity of Aging Airplanes*, edited by S. N. Atluri, S. G. Sampath, and P. Tong, Springer-Verlag, Berlin, 1991.

[2]Schijve, J., "Multiple-Site Damage in Aircraft Fuselage Structures," *Fatigue and Fracture of Materials and Structures*, Vol. 18, No. 3, 1995, pp. 329–344.

[3]Newman, J. C., Jr., Dawicke, D. S., Sutton, M. A., and Bigelow, C. A., "A Fracture Criterion for Widespread Cracking in Thin-Sheet Aluminum Alloys," Durability and Structural Integrity of Airframes, 17th International Committee on Aeronautical Fatigue Symposium, Stockholm, Sweden, 1993.

[4]Park, J. H., Singh, R., Pyo, C. R., and Atluri, S. N., "Structural Integrity of Fuselage Panels with Multisite Damage," *Journal of Aircraft*, Vol. 32, No. 3, 1995, pp. 656–662.

[5]Dugdale, D. S., "Yielding of Steel Sheets Containing Slits," *Journal of the Mechanics and Physics of Solids*, Vol. 8, No. 2, 1960, pp. 100–104.

[6]Swift, T., "Damage Tolerance Capability," *Fatigue of Aircraft Materials*, Delft Univ. Press, Delft, The Netherlands, 1992, pp. 351–387.

[7]Broek, D., Jeong, D. Y., and Thompson, D., "Testing and Analysis of Flat and Curved Panels with Multiple Cracks." *Advanced Structural Integrity Methods for Airframe Durability and Damage Tolerance*, NASA CP 3274, 1994, pp. 87–98.

[8]Cai, H., and Faber, K. T., "On the Use of Approximation Method for Microcrack Shielding Problems," *Journal of Applied Mechanics*, Vol. 59, No. 3, 1992, pp. 479–501.

[9]Kuang, J. H., and Chen, C. K., "The Failure of Ligaments due to Multiple-Site Damage Using Interactions of Dugdale Type Cracks," *Fatigue and Fracture of Materials and Structures*, Vol. 21, No. 9, 1998, pp. 1147–1157.

[10]Tada, H., Paris, P. C., and Irwin, G. R., *The Stress Analysis of Cracks Handbook*, 2nd ed., Paris Productions Inc. and Del Research Corp., St. Louis, MO, 1985.

[11]Hoysan, S. F., and Sinclair, G. B., "On the Variability of Fracture Toughness," *International Journal of Fracture*, Vol. 60, No. 3, pp. R43–R49.

[12]Jeong, D. Y., and Brewer, J. C., "On the Linkup of Multiple Cracks," *Engineering Fracture Mechanics*, Vol. 51, No. 2, 1995, pp. 233–238.